AIAA JOURNAL
Vol. 48, No. 5, May 2010

Introduction to the Bayesian Approach Applied to Elastic Constants Identification

Christian Gogu*
Ecole des Mines de Saint Etienne, 42023 Saint Etienne, France
Raphael Haftka†
University of Florida, Gainesville, Florida 32611
and
Rodolphe Le Riche,‡ Jérôme Molimard,§ and Alain Vautrin¶
Ecole des Mines de Saint Etienne, 42023 Saint Etienne, France

DOI: 10.2514/1.40922

The basic formulation of the least-squares method, based on the L_2 norm of the residuals, is still widely used today for identifying elastic constants of aerospace materials from experimental data. While this method often works well, methods that can benefit from statistical information, such as the Bayesian method, may sometimes be more accurate. We seek situations with significant difference between the material properties identified by the two methods. For a simple three-bar truss example we illustrate three situations in which the Bayesian approach systematically leads to more accurate results: different sensitivity of the measured response to the parameters to be identified, different uncertainty in the measurements, and correlation among response components. When all three effects add up, the Bayesian approach can be much more accurate. Furthermore, the Bayesian approach has the additional advantage of providing the uncertainty in the identified parameters. We also compare the two methods for a more realistic problem of identification of elastic constants from natural frequencies of a composite plate.

I. Introduction

CURRENT design of aerospace structures tends to increasingly consider uncertainty in material properties. Variability in strength, for example, is now used to define the A-basis or B-basis design allowable [1], to comply with regulations of the Federal Aviation Administration. Uncertainty in elastic constants due to measurement and modeling errors is an important component of the total uncertainty.

Currently, a very widespread method for elastic constants identification seeks to minimize the least-squares error between the experimental data and the model predictions. In spite of the existence of advanced least-squares formulations, which take into account statistical information [2–4], the simplest formulations of the least-squares method, based on minimizing the L_2 norm of the residual [2], are still extensively used today [5–12]. This basic nonstatistical least-squares formulation is very simple and most often leads to reasonably accurate results. In some situations, however, using statistical identification frameworks may lead to significant improvements in accuracy.

The objective of the present paper is to identify and illustrate such situations. As the statistical method we chose the Bayesian approach, which is among the most general statistical approaches, while its formulation remains relatively simple. Isenberg [13] detailed a Bayesian framework for parameter estimation in 1979, which was later applied by others, in particular, to frequency or modal identification, i.e., identifying material properties from vibration test data [14–19]. The Bayesian method has also been proposed for model validation and verification [20,21].

To compare the results of the basic least-squares and the Bayesian identification, we used simulated experiments on two problems: a three-bar truss problem and a plate-vibration problem. We made the choice of simulated experiments, since these allow easier repeatability and more flexibility in isolating different factors that affect the identification, thus helping to determine the most influential ones. In [22] we provide the results of the Bayesian identification of elastic constants from actual vibration measurements, and identification from full field displacement measurements is provided in [23].

In Sec. II we provide a brief theoretical overview of the methods used. Section III introduces a three-bar truss identification problem, which also serves as a tutorial for the Bayesian approach. In Sec. IV we compare the Bayesian and the least-squares approaches for the three-bar truss, identifying situations that differ significantly in the results. Section V compares the two identification methods on a more complex, vibration-based problem. In Sec. VI we provide some concluding remarks.

II. Least-Squares and Bayesian Methodologies to Parameter Identification

A. Least-Squares Formulations

The most common least-squares approach to parameter identification finds the parameters that minimize the squared error between experimental observations and model predictions.

Let $\boldsymbol{x}$ be a vector of n material properties that we seek to identify, and let $\boldsymbol{y}^{\text{meas}}$ be a vector of m experimental measurements. We assume that we have a mathematical model relating $\boldsymbol{x}$ to predictions of $\boldsymbol{y}$ such that $\boldsymbol{y}(\boldsymbol{x})$ is the vector of m model predictions. Note that $\boldsymbol{y}$ is usually also a function of parameters $\boldsymbol{p}$ other than material properties (geometry, loads, etc.), which are usually fixed during least-squares identification.

Received 12 September 2008; accepted for publication 5 February 2010.

*Currently Postdoctoral Teaching and Research Assistant, Institut Clément Ader, Université de Toulouse, 118 Route de Narbonne, 31062 Toulouse, France; christian.gogu@gmail.com. Student Member AIAA (Corresponding Author).

†Distinguished Professor, Department of Mechanical and Aerospace Engineering, P.O. Box 116250. Fellow AIAA.

‡Permanent Research Associate, 158 Cours Fauriel; Centre National de la Recherche Scientifique.

§Associate Professor, Centre Sciences des Matériaux et des Structures, Laboratoire des Tribologie et Dynamique des Systèmes.

¶Professor, Centre Sciences des Matériaux et des Structures, Laboratoire des Tribologie et Dynamique des Systèmes.

The simplest least-squares formulation minimizes the objective function $J(\boldsymbol{x})$ defined in Eq. (1) to obtain the identified properties ([2], chapter 1):

$$J(\boldsymbol{x}) = \frac{1}{2}(\boldsymbol{y}(\boldsymbol{x}) - \boldsymbol{y}^{\text{meas}})^T(\boldsymbol{y}(\boldsymbol{x}) - \boldsymbol{y}^{\text{meas}}) = \frac{1}{2}\sum_{i=1}^{m}(y_i(\boldsymbol{x}) - y_i^{\text{meas}})^2 \tag{1}$$

A more general least-squares formulation uses $C(\boldsymbol{x})$, the variance–covariance matrix of $y(\boldsymbol{x})$, as weighting and minimizes

$$J(\boldsymbol{x}) = \tfrac{1}{2}(\boldsymbol{y}(\boldsymbol{x}) - \boldsymbol{y}^{\text{meas}})^T C(\boldsymbol{x})^{-1}(\boldsymbol{y}(\boldsymbol{x}) - \boldsymbol{y}^{\text{meas}}) \tag{2}$$

thus taking statistical information into account. The variance–covariance structure is assumed based on empirical evidence or calculated using a model.

Because of the challenge of constructing a realistic variance–covariance matrix $C(\boldsymbol{x})$, most least-squares identification applications revert to the use the formulation of Eq. (1), which ignores potential statistical information. The formulation of Eq. (1) or its normalized version, which we call the basic least-squares in the rest of the paper, have been recently used, for example, in the domain of elastic constants identification from full field strain measurements [5–8] or from vibration data [9–12].

B. Bayesian Method

The Bayesian identification approach is a statistical approach. Unlike the least-squares identification method, it will not provide a single value for the identified parameter, but a probability distribution. The unknown material properties have a single value, but it is unknown, and their possible values are represented by the random variable $\boldsymbol{X}$ (with $\boldsymbol{x}$ being an instance of $\boldsymbol{X}$). Its probability density function (PDF) is denoted as $\pi_X(\boldsymbol{x})$. In Bayesian identification we seek to identify the distribution of the material properties $\boldsymbol{X}$ given a vector of measurements $\boldsymbol{y}^{\text{meas}}$. The vector of measurements is assumed to be contaminated by a vector of unknown measurement errors $\boldsymbol{e}^{\text{meas}}$, stemming from the random variable $\boldsymbol{\Sigma}^{\text{meas}}$. The true, but unknown, response is then given by $\boldsymbol{y}_{\text{true}}^{\text{meas}} = \boldsymbol{y}^{\text{meas}} - \boldsymbol{e}^{\text{meas}}$. Letting $\boldsymbol{Y}_{\text{true}}^{\text{meas}}$ be the random variable of the true response value (it is a random variable because $\boldsymbol{y}_{\text{true}}^{\text{meas}}$ is unknown), we can then write

$$\boldsymbol{Y}_{\text{true}}^{\text{meas}} = \boldsymbol{y}^{\text{meas}} - \boldsymbol{\Sigma}^{\text{meas}} \tag{3}$$

For the identification we compare the measurements to a model's prediction (e.g., finite element model) $\boldsymbol{y}_{p0}(\boldsymbol{x})$ that is a function of the material properties $\boldsymbol{x}$ and other input parameters $\boldsymbol{p}$ (e.g., geometry, loading) taken at their values $\boldsymbol{p}_0$. Because of modeling error, and because the input parameters may not be accurately known, the random variable of the true response is given as

$$\boldsymbol{Y}_{\text{true}}^{\text{model}}(\boldsymbol{x}) = \boldsymbol{y}_{p0}(\boldsymbol{x}) - \boldsymbol{\Sigma}^{\text{model}} \tag{4}$$

where $\boldsymbol{\Sigma}^{\text{model}}$ is the random variable of the error due to modeling uncertainty and uncertainty in the input parameters $\boldsymbol{p}$.

Bayesian identification involves calculating, for given material properties $\boldsymbol{x}$, the likelihood that the true response is the same whether derived from the measurement or from the model (i.e., the likelihood that $\boldsymbol{Y}_{\text{true}}^{\text{meas}} = \boldsymbol{Y}_{\text{true}}^{\text{model}}$) equality, which can also be written

$$\boldsymbol{D} = \boldsymbol{Y}_{\text{true}}^{\text{model}} - \boldsymbol{Y}_{\text{true}}^{\text{meas}} = \boldsymbol{0} \tag{5}$$

This likelihood, denoted as $l(\boldsymbol{x})$, is then defined as the probability density function of $\boldsymbol{D}$, given that $\boldsymbol{X} = \boldsymbol{x}$ (denoted as $\boldsymbol{D}/\boldsymbol{X} = \boldsymbol{x}$), taken at zero: $l(\boldsymbol{x}) = \pi_{D/X=x}(\boldsymbol{0})$. Here, as in the rest of the paper, π stands for probability density function. While the subscript of π can represent directly the random variable of the PDF as in $\pi_X(\boldsymbol{x})$, it can stand, as here, for the conditional random variable $\boldsymbol{D}$, given that $\boldsymbol{X} = \boldsymbol{x}$ (denoted as $\boldsymbol{D}/\boldsymbol{X} = \boldsymbol{x}$).

It is important to note that the PDF of $\boldsymbol{D}$, given $\boldsymbol{X} = \boldsymbol{x}$, is a distribution in terms of the values of $\boldsymbol{D}$ and that $\boldsymbol{x}$ can be seen as a parameter of this distribution. That is, for a given material properties value $\boldsymbol{x}$, we need to determine the distribution of $\boldsymbol{D}$. The likelihood will then be this PDF of $\boldsymbol{D}$ for the given $\boldsymbol{x}$, taken at $\boldsymbol{D} = \boldsymbol{0}$. It becomes a function of $\boldsymbol{x}$ when considered for all possible values of the material properties, called the likelihood function of $\boldsymbol{x}$ given the measurements and denoted as $l(\boldsymbol{x})$.

An alternative formulation for calculating the likelihood function can be achieved by introducing the random variable $\boldsymbol{Y}$ of the measurement prediction for a given $\boldsymbol{x}$:

$$\boldsymbol{Y}(\boldsymbol{x}) = \boldsymbol{y}_{p0}(\boldsymbol{x}) - \boldsymbol{\Sigma}^{\text{model}} + \boldsymbol{\Sigma}^{\text{meas}} \tag{6}$$

Equation (5) can then be written as $\boldsymbol{Y} = \boldsymbol{y}^{\text{meas}}$ and the likelihood function of $\boldsymbol{x}$, given that the measurement prediction $\boldsymbol{Y}$ should be equal to the actual measurement $\boldsymbol{y}^{\text{meas}}$, is then

$$l(\boldsymbol{x}) = \pi_{Y/X=x}(\boldsymbol{y}^{\text{meas}}) \tag{7}$$

For each $\boldsymbol{x}$, the likelihood value is the PDF of the measurement prediction given the material properties, $\boldsymbol{Y}/\boldsymbol{X} = \boldsymbol{x}$, taken at the point of the actually measured response $\boldsymbol{y}^{\text{meas}}$.

In the rest of the paper we will use this second formulation, involving the random variable of the measurement prediction, which is the most common formulation used in Bayesian identification literature. Note, though, that most studies traditionally simply call $\boldsymbol{Y}$ the random variable of the measurements. We preferred calling it the measurement prediction, since it is constructed for any $\boldsymbol{x}$ (not just the true value of the properties) and because it can include modeling uncertainty $\boldsymbol{\Sigma}^{\text{model}}$.

Briefly, note that the first formulation allows us to take advantage of the independence of the random variables $\boldsymbol{Y}_{\text{true}}^{\text{meas}}$ and $\boldsymbol{Y}_{\text{true}}^{\text{model}}$ in order to reduce the computational cost of Monte Carlo simulations, which may be required to propagate uncertainties through the model. Since we do not consider expensive problems in this paper, we will not detail this further, but refer the reader to [23].

An advantage of the Bayesian approach is that it can not only account for the measurements through the likelihood function, but it can also easily account for prior knowledge on the material properties using the prior distribution $\pi_X^{\text{prior}}(\boldsymbol{x})$, i.e., the PDF of $\boldsymbol{X}$ before observing $\boldsymbol{y}^{\text{meas}}$. Such prior knowledge can come from manufacturer's specifications or previous tests.

Based on the likelihood function and the prior distribution, Bayes's rule then gives $\pi_{X/Y=y^{\text{meas}}}(\boldsymbol{x})$, the PDF of $\boldsymbol{X}$ given that the measurement prediction $\boldsymbol{Y}$ should be equal to $\boldsymbol{y}^{\text{meas}}$, by the product of the likelihood function by the prior distribution:

$$\pi_{X/Y=y^{\text{meas}}}(\boldsymbol{x}) = \tfrac{1}{K}\cdot l(\boldsymbol{x})\cdot \pi_X^{\text{prior}}(\boldsymbol{x}) = \tfrac{1}{K}\cdot \pi_{Y/X=x}(\boldsymbol{y}^{\text{meas}})\cdot \pi_X^{\text{prior}}(\boldsymbol{x}) \tag{8}$$

where K denotes a normalizing constant.

The identified PDF, $\pi_{X/Y=y^{\text{meas}}}(\boldsymbol{x})$, also called posterior distribution, can be characterized by the mean and most likely values as well as by the variance–covariance matrix, thus providing uncertainty measures in the identified properties, which are usually not obtained in studies applying the basic least-squares approach. For additional details on the theory of Bayesian analysis, we also refer the reader to [24,25].

III. Three-Bar Truss Didactic Example

A. Description of the Three-Bar Truss Example

We consider a three-bar truss, subject to a horizontal force p and a vertical force r, as shown in Fig. 1. All three bars have the same Young's modulus E of 10 GPa, which is unknown and which we want to identify from strain measurements on two or three of the bars. The cross-sectional areas of the bars are known exactly: A_A is the cross-sectional area of bars A and C, and A_B is the cross-sectional area of bar B. From static analysis we find the following relationships for the strains in the bars.

$$\varepsilon_A = \frac{1}{E}\left(\frac{r}{4A_B + A_A} + \frac{p}{\sqrt{3}A_A}\right) \tag{9}$$

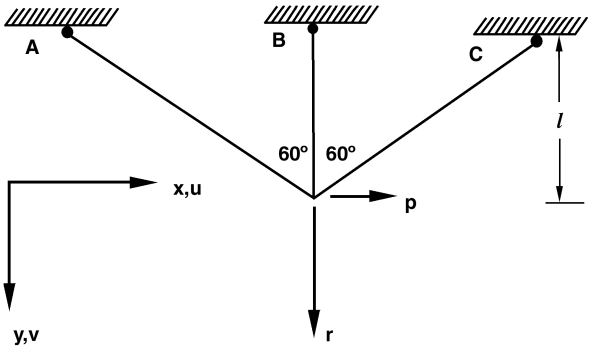

Fig. 1 Three-bar truss problem.

$$\varepsilon_C = \frac{1}{E}\left(\frac{r}{4A_B + A_A} - \frac{p}{\sqrt{3}A_A}\right) \tag{10}$$

$$\varepsilon_B = \frac{1}{E}\frac{4r}{4A_B + A_A} \tag{11}$$

B. Sources of Uncertainty

We consider that due to measurement error, the measured values of the forces p and r might not be their true values. We assume that the measured forces are normally distributed with mean values of 10^4 N for p and 10^5 N for r and a standard deviation of 500 N for both.

Note that we ignore other sources of uncertainty in the problem, such as uncertainties in the strain measurements and cross-sectional measurements. This simplification allows us to easily identify situations in which the Bayesian and basic least-squares identifications significantly differ in results. Assuming uncertainties only on the forces was a reasonable compromise between simplicity and flexibility for identifying such situations. The vibration identification problem we consider in the second part provides a more complex situation.

C. Least-Squares Method

Assuming that we measure the strains in bars A and B, the least-squares objective function of Eq. (1) can be written as

$$J(E) = \tfrac{1}{2}((\varepsilon_A(E) - \varepsilon_A^{\text{meas}})^2 + (\varepsilon_B(E) - \varepsilon_B^{\text{meas}})^2) \tag{12}$$

Note that even though the loads p and r are uncertain, we have to provide a single nominal value for each. The most natural candidates are the means of p and r. Note also that in this simple case it was possible to find the minimum of $J(E)$ analytically.

D. Bayesian Method

Applying Eq. (8) to the three-bar truss problem we can write the distribution of the Young's modulus of the bars given that we measured $\varepsilon_A^{\text{meas}}$ and $\varepsilon_B^{\text{meas}}$ in bars A and B, respectively, as shown in Eq. (13):

$$\pi_{E/\{\varepsilon_A,\varepsilon_B\}=\{\varepsilon_A^{\text{meas}},\varepsilon_B^{\text{meas}}\}}(E) = \tfrac{1}{K}\pi_{\{\varepsilon_A,\varepsilon_B\}/E}(\{\varepsilon_A^{\text{meas}}, \varepsilon_B^{\text{meas}}\}) \cdot \pi_E^{\text{prior}}(E) \tag{13}$$

The right-hand side of this equation is composed, apart from the normalization constant K, of two quantities. The first is the likelihood function of E given the measurements and the other is the prior probability distribution of E. Here, we assume that the prior knowledge is in the form of a truncated normal distribution with a mean value of 9.5 GPa and a standard deviation of 1.5 GPa. We truncate the distribution at 8 and 11 GPa, meaning that we consider it impossible for the properties to lie outside these bounds. This is a wide prior, meaning that its standard deviation is significantly larger than that of the likelihood function that will be obtained for this problem, implying that the effect of the prior will be negligible. In the present paper, we choose not to concentrate on investigating the effect of the prior, thus the choice of a wide prior, centered relatively far away from the true value of 10 GPa to avoid significantly biasing our comparison in favor of the Bayesian identification. Brief results on the impact of the prior will be given in Sec. IV.E.

The other right-hand side term in Eq. (13) is the likelihood function of E given the measurements $\varepsilon_A^{\text{meas}}$ and $\varepsilon_B^{\text{meas}}$. It provides an estimate of the likelihood of different modulus values given the test results. In general, we vary E successively from $-\infty$ to ∞, in order to calculate $\pi_{\{\varepsilon_A,\varepsilon_B\}/E}(\{\varepsilon_A^{\text{measure}}, \varepsilon_B^{\text{measure}}\})$ for each E value. Here, because the likelihood function multiplies the truncated prior, we need to consider only values in the truncated region. For a given E we have a PDF for the strains, due to the uncertainty in the loads p and r, which propagates to the strains. This PDF is then evaluated at the point $\{\varepsilon_A, \varepsilon_B\} = \{\varepsilon_A^{\text{meas}}, \varepsilon_B^{\text{meas}}\}$.

This procedure is repeated for a series of E values within the truncation bounds, thus constructing the likelihood function point by point, then the posterior PDF [left-hand side of Eq. (13)] by the produce of the prior distribution by the likelihood function. Appendix A provides a tutorial description of the Bayesian procedure applied to the three-bar truss problem.

Note that computational cost was not an issue here, due to the simplicity of the problem, but it can increase significantly as m (the number of experimental values) and n (the number of parameters to be identified) increase. The major part of the computational cost is the propagation of uncertainties through the model. If more complex models were used (e.g., finite elements), the cost could even become prohibitive without the use of approximations (e.g., response-surface approximations [26]) or more advanced simulation techniques (e.g., the use of the independence of the different sources of uncertainty in combination with the conditional-expectation method [27] and Markov chain Monte Carlo simulation [4]). The aforementioned methods usually allow bringing the computational cost down to reasonable levels for many real-life problems, but still significantly higher than that of the basic least-squares method. This is the price to pay, however, for using statistical information in input and obtaining the statistics of the identified parameters with arbitrary (not necessarily Gaussian) probability distributions.

IV. Comparison of Least-Squares and Bayesian Approaches for the Three-Bar Truss Problem

A. Comparison Method

The results of both the least-squares and Bayesian approaches depend on the actual, but unknown, values of the loads p and r in an experiment. We first (Secs. IV.B–IV.E) compare the two methods for extreme cases in which the actual values of p and r are two standard deviations away from their mean values: $p_{\text{true}} = p_m + 2\sigma_p$ and $r_{\text{true}} = r_m - 2\sigma_m$. These accentuate the difference between the two methods. Then in Sec. IV.F, we consider 1000 repetitions of the identification processes in which the true values of p and r are obtained by Monte Carlo simulations from their distributions. This second case compares the average accuracy of the methods measured by the dispersion (e.g., standard deviation) in the modulus estimate as the loads are varied.

For all cases we compare the modulus obtained from the least-squares approach to the most likely value from the Bayesian probability distribution. The differences between the two methods are likely to be influenced by three factors: 1) differences in the sensitivity of strains to Young's modulus, 2) differences in the uncertainty of the different strains, and 3) correlation between strains. For points 1 and 2, we use the three bars truss with strain measurements on two of the bars, and for point 3, we use measurements on all three bars.

B. Results for Different-Sensitivity Strains

Here, we create a situation in which the strain in bar A is more sensitive to Young's modulus variations than the strain in bar B. The least-squares approach tends to emphasize high-sensitivity data (see Appendix B). Since all strains are inversely proportional to Young's modulus, the sensitivity of the strain is proportional to the strain's magnitude. A high strain (in absolute value) in one bar means that the

Table 1 Numerical values for different-sensitivity strains

	Input parameters				Strains	
Parameter	A_A, m^2	A_B, m^2	p, N	r, N	ε_A, mm/m	ε_B, mm/m
Mean value	2×10^{-4}	1×10^{-2}	10^4	10^5	3.13	0.995
Standard deviation	——	——	250	2500	0.0725	0.0248
Measured strains[a]	——	——	——	——	3.26	0.945

[a]Extreme case obtained from Eqs. (9) and (11) with $E = 10$ GPa, $p = p_{\text{mean}} + 2\sigma_p$, and $r = r_{\text{mean}} - 2\sigma_m$.

strain in that bar has a high sensitivity to E. Thus, we provide the magnitude of the strains as a measure of their sensitivity to E.

We use the values in Table 1 to create a strain in bar A that is about triple that in bar B (hence three times more sensitive). The same relative uncertainty in the loads is applied (2.5%), which propagates to about the same relative uncertainty in ε_A and ε_B.

The results of the two identification procedures are presented in Table 2. We also provide the Young's modulus that would be obtained with each of the measurements alone by inverting Eqs. (9) and (11). The relatively poor results of the least-squares method are obtained because it implicitly assigns more weight to $\varepsilon_A^{\text{meas}}$, to which E is more sensitive.

Normalizing the strain residue with respect to the measured strains would seem to be an obvious solution to this problem. However, while it indeed solves the variable magnitude issue, it can create another problem by assigning the same weights to strains that have very different uncertainties, which may lead to inaccurate results, as will be shown in the next section. This means that it is risky to perform normalization without taking into account the uncertainties in the measurements.

C. Results for Different Uncertainty in the Strains

To create different uncertainty in the two strains, we used the values given in Table 3. To isolate this effect from the previous one, the calculated strains have about the same magnitude and thus the same sensitivity to E. We chose 5% uncertainty in p and 0.5% in r, which results in ε_A having about seven times higher uncertainty than ε_B. The results of the two identification procedures are presented in Table 4 for the extreme case.

Again, the Bayesian approach is much more accurate than the least-squares approach. Since the two strains have about the same sensitivity to E (due to same magnitude), the least-squares approach assigns about the same weight to each, so the identified E is about the average between the E found with each measurement alone. The uncertainty information is taken into account by the Bayesian method through the likelihood function, which may be viewed as assigning more weight to the measurement having low uncertainty. This explains why the Bayesian-identified modulus is much closer to the one found using $\varepsilon_B^{\text{meas}}$ alone. For additional explanations and graphical representation of the results, refer to Appendix C.

D. Results for Correlation Among the Responses

To show the effect of correlation, we need three strain measurements, with two strongly correlated, but not correlated to the third. For this purpose, we used the values in Table 5. To isolate this effect from the previous one, we have the same relative uncertainty in p and in r, which propagates to about the same relative uncertainty in all three strains. We could not, however, find values that lead to the same magnitude for all three strain measurements. Therefore, the least-squares approach will pay less attention to the small $\varepsilon_B^{\text{meas}}$. The

Table 2 Extreme case identification results for different-sensitivity strain (true value of modulus is 10 GPa)

	From $\varepsilon_A^{\text{meas}}$ alone	From $\varepsilon_B^{\text{meas}}$ alone	Least-squares	Bayesian
E, GPa	9.59	10.52	9.67	9.97 (most likely value), 0.174 (standard deviation)

Table 3 Numerical values for variable response uncertainty

	Input parameters				Strains	
Parameter	A_A, m^2	A_B, m^2	p, N	r, N	ε_A, mm/m	ε_B, mm/m
Mean value	7.85×10^{-4}	1×10^{-2}	10^4	10^5	0.980	0.980
Standard deviation	——	——	500	500	0.0368	0.0049
Measured strains[a]	——	——	——	——	1.05	0.970

[a]Extreme case obtained from Eqs. (9) and (11) with $E = 10$ GPa, $p = p_{\text{mean}} + 2\sigma_p$, and $r = r_{\text{mean}} - 2\sigma_m$.

Table 4 Extreme case identification results for different response uncertainty (true value of E is 10 GPa)

	From $\varepsilon_A^{\text{meas}}$ alone	From $\varepsilon_B^{\text{meas}}$ alone	Least-squares	Bayesian
E, GPa	9.32	10.10	9.69	10.08 (most likely value) 0.058 (standard deviation)

Table 5 Numerical values for response correlation

	Input parameters				Strains		
Parameter	A_A, m^2	A_B, m^2	p_m, N	r_m, N	ε_A, mm/m	ε_B, mm/m	ε_C, mm/m
Mean value	2×10^{-4}	1×10^{-2}	10^4	10^5	3.13	0.995	−2.64
Standard deviation	——	——	250	2500	0.0725	0.0248	0.0725
Measured strains[a]	——	——	——	——	3.27	0.945	−2.79

[a]Extreme case obtained from Eqs. (9) and (11) with $E = 10$ GPa, $p = p_{\text{mean}} + 2\sigma_p$, and $r = r_{\text{mean}} - 2\sigma_m$.

correlation between ε_A and ε_C is -0.985, whereas the correlation between the other two couples is 0.086, meaning that only ε_A and ε_C are highly correlated.

Since the present case will also be affected by the different magnitude of the strains, we compare Tables 2 and 6, in which $\varepsilon_B^{\text{meas}}$ is small for both. Their comparison shows that the least-squares method is more affected by adding a correlated measurement (+0.9% difference) than is the Bayesian approach (+0.1% difference). The explanation is that the least-squares approach treats all three measurements as independent and, due to the small magnitude of $\varepsilon_B^{\text{meas}}$, it mainly averages $\varepsilon_A^{\text{meas}}$ and $\varepsilon_C^{\text{meas}}$. The Bayesian approach may be viewed as averaging the highly correlated $\varepsilon_A^{\text{meas}}$ and $\varepsilon_C^{\text{meas}}$ first, then, considering the average value as a single experiment, it combines it with the uncorrelated one.

E. Results for All Three Effects Together

In the last case we combine all three effects, which is what would happen when having different strain sensitivities and uncertainties, as well as strong correlation between the measurements. As before, we analyze an extreme case here, meaning that we choose numerical values such that the different effects add up, to magnify the difference between the two identification approaches. The numerical values used are given in Table 7. The correlation between ε_A and ε_C is -0.999, between ε_A and ε_B it is 0.014, and between ε_B and ε_C it is 0.002.

We can see in Table 8 that in this case the error in the least-squares approach is exacerbated. All effects act together and against the least-squares method. On the other hand, the Bayesian method considers almost only ε_B, which has, by far, the lowest uncertainty, leading the Bayesian method to be much closer to the true Young's modulus.

We now briefly discuss the influence of the prior distribution on the Bayesian identification results. The previous results were obtained for a truncated normally distributed wide prior with a mean value 9.5 GPa and a large standard deviation of 1.5 GPa. If we change the standard deviation of the prior distribution to 0.75 GPa, keeping the same mean and the same truncation bounds, we obtain a most likely value of 10.07 GPa (10.08 previously, see Table 8) for this extreme case, which is a small improvement, due to a narrower prior. If we change the mean of the prior distribution to 10.5 GPa, keeping the standard deviation and the truncation bounds the same, we obtain a most likely value of 10.09 GPa (compared to 10.08). So, even though we changed the prior significantly, it had very small effects on the Bayesian identification results. Of course, a much narrower, more accurate, prior distribution would have substantially improved the accuracy. Since the availability of a narrow prior is, however, always problem-specific, we chose to work with a wide prior here, to avoid significantly biasing the comparison on the basis of the prior.

F. Average Performance

To complement the results obtained for the extreme case, we repeat the previous procedure 1000 times for random values of the loads obtained by Monte Carlo simulation, instead of for extreme values. The numerical values for the cross sections, the loads, and their uncertainty are those given earlier for each case. The accuracy of the methods will be measured by the standard deviation of E as the loads are varied (see Table 9). For the individual cases the standard deviations of the Bayesian approach are lower by a fraction (different-sensitivity case) to a factor of 3.5 (different uncertainty). The difference is even more striking for the three effects combined, since the E found by the Bayesian approach will be, on average, almost 10 times closer to the true value.

Of course, depending on the luck of the draw, we could very well find an experiment for which the least-squares identified modulus is more accurate than the Bayesian modulus. However, the average results show that the situations illustrated on the extreme cases are not just bad luck, but are representative of a systematic error, due to the inappropriate treatment of normalization, uncertainties, and correlation by the basic least-squares approach.

On a final note, for the previously analyzed cases, the results obtained by the Bayesian method can also be obtained by the generalized least-squares formulation of Eq. (2). For more complex problems though, the Bayesian approach has the advantage of easily handling non-Gaussian uncertainties through Monte Carlo simulation, as will be illustrated with the vibration problem. Also, even though not studied here, a main remaining advantage of the Bayesian approach over the generalized least-squares formulations is the simplicity of taking into account prior information. In our examples we chose a wide prior though, to concentrate on the comparison between the basic least-squares and the statistical Bayesian approaches.

V. Vibration Identification Problem

A. Description of the Problem

In this section we explore how the two methods compare for a more complex identification problem of determining the elastic properties from the natural frequencies of a composite plate. Since

Table 6 Extreme case identification results for response correlation (true value of E is 10 GPa)

	From $\varepsilon_A^{\text{meas}}$	From $\varepsilon_B^{\text{meas}}$	From $\varepsilon_C^{\text{meas}}$	Least-squares	Bayesian
E, GPa	9.59	10.52	9.43	9.58	9.96 (most likely value) 0.196 (standard deviation)

Table 7 Numerical values for the three combined effects

	Input parameters				Strains		
Parameter	A_A, m^2	A_B, m^2	p, N	r, N	ε_A, mm/m	ε_B, mm/m	ε_C, mm/m
Mean value	2×10^{-4}	1×10^{-2}	10^4	10^5	3.13	0.995	−2.64
Standard deviation	——	——	500	500	0.144	0.005	0.144
Measured strains[a]	——	——	——	——	3.42	0.985	−2.93

[a]Extreme case obtained from Eqs. (9) and (11) with $E = 10$ GPa, $p = p_{\text{mean}} + 2\sigma_p$ and $r = r_{\text{mean}} - 2\sigma_m$.

Table 8 Extreme case identification results for the three combined effects (true value of the E is 10 GPa

	From $\varepsilon_A^{\text{meas}}$	From $\varepsilon_B^{\text{meas}}$	From $\varepsilon_C^{\text{meas}}$	Least-squares	Bayesian
E, GPa	9.16	10.10	9.00	9.14	10.08 (most likely value) 0.058 (standard deviation)

Table 9 Average performance of the methods in the different cases (the differences in the mean mainly reflects the limited sample size of 1000 cases)

	Mean of E, GPa	Standard deviation of E, GPa
Different sensitivity		
Least-squares	10.01	0.200
Bayesian	9.99	0.167
Different uncertainty		
Least-squares	10.00	0.178
Bayesian	9.99	0.051
Correlation		
Least-squares	10.01	0.221
Bayesian	9.99	0.167
All three together		
Least-squares	10.04	0.447
Bayesian	9.99	0.050

Table 10 True values of the laminate elastic constants

	Parameter			
	E_x	E_y	G_{xy}	ν_{xy}
True value	57.6 GPa	57.6 GPa	4.26 GPa	0.05

Table 11 Assumed uncertainties on the input parameters

	Parameter			
	a, mm	b, mm	h, mm	ρ, kg/m^3
Mean value	200	250	3	1536
Standard deviation	0.5	0.5	0.01	7.67

we are only interested here in comparing the two methods, we simulate experiments from analytical expressions available for simply supported plates and error models explained hereafter.

We consider a $[0, 90]_s$ simply supported graphite/epoxy composite laminate of dimensions $a = 200$ mm and $b = 250$ mm and of total thickness $h = 3$ mm. The true elastic constants of the laminate are given in Table 10. We aim to identify these properties of the laminate and not those of an individual ply. For simplicity and easy graphical representation we identify only two properties, assuming that ν_{xy} is known as well as $E_x = E_y$. This leaves E_x and G_{xy} to be identified. Note, however, that the procedure described would remain the same if all four properties would be identified.

The simulated experiment consists of measuring the first nine natural frequencies of the plate. The measured frequencies are generated from a model, to which we add various sources of uncertainty such as measurement and modeling errors, detailed in the next section. Thin-plate theory is used as a model for obtaining the frequency of the mode (k, l) in terms of density ρ and rigidities D_{ij}, as shown in Eq. (14). The bending rigidities D_{ij} are a function of the thickness and the individual in-plane properties of the laminate (longitudinal and transverse Young's moduli E_x and E_y, Poisson's ratio ν_{xy}, and shear modulus G_{xy}). For the detailed construction procedure of the rigidities of a composite laminate, refer to [28] (chapter 2.3).

Table 13 Least-squares and Bayesian results for a randomly simulated particular case

	E_x, GPa	G_{xy}, GPa
True values	57.6	4.26
Least-squares values	56.9	4.66
Bayesian most likely values	57.9	4.30

$$f_{kl} = \frac{\pi}{2\sqrt{\rho h}} \sqrt{D_{11}\left(\frac{k}{a}\right)^4 + 2(D_{12} + 2D_{66})\left(\frac{k}{a}\right)^2\left(\frac{l}{b}\right)^2 + D_{22}\left(\frac{l}{b}\right)^4} \tag{14}$$

B. Sources of Uncertainty

For this problem we considered uncertainty in input parameters, measurement uncertainty, and modeling error. For the model input parameters, denoted as $\boldsymbol{p}$, we assumed normally distributed, uncorrelated uncertainties (see Table 11). We combine the measurement error and modeling error into a uniformly distributed error, within an interval, which increases linearly for the higher natural frequencies, because higher modes have shorter wavelengths and are less well modeled by thin-plate theory. The measured frequencies are then simulated using the following equation:

$$f_{kl}^{\text{meas}} = f_{kl}^{\text{resp}}(\{E_x, G_{xy}\}^{\text{true}}, \boldsymbol{p}^{\text{true}}) + u_{kl} \tag{15}$$

where f^{resp} is obtained from Eq. (14), which is a function of $\{E_x, G_{xy}\}^{\text{true}}$, the true values of the material properties, and $\boldsymbol{p}^{\text{true}}$, which are the true values of the other input parameters a, b, h, and ρ. The random variable u_{kl} aggregates the modeling and measurement uncertainties $\boldsymbol{\Sigma}^{\text{model}}$ and $\boldsymbol{\Sigma}^{\text{meas}}$ of Eq. (6) into a single quantity. It is assumed to be uniformly distributed in the interval $[a_{kl}, b_{kl}]$, where

$$\begin{aligned} a_{kl} &= f_{11}^{\text{resp}}\left(a_{lb} + a_{ub}\frac{k+l-2}{k_{\max}+l_{\max}-2}\right) \\ b_{kl} &= f_{11}^{\text{resp}}\left(b_{lb} + b_{ub}\frac{k+l-2}{k_{\max}+l_{\max}-2}\right) \end{aligned} \tag{16}$$

For nine frequencies $k_{\max} = l_{\max} = 3$. We chose $a_{lb} = -2.5 \times 10^{-3}$, $a_{ub} = -4 \times 10^{-2}$, $b_{lb} = 2.5 \times 10^{-3}$, and $b_{ub} = -2 \times 10^{-2}$. With these numerical values the error for the lowest natural frequency f_{11} would be uniformly distributed within the bounds $[-0.0025 f_{11}, 0.0025 f_{11}]$. The error for the highest (ninth) natural frequency measured would be uniformly distributed within the bounds $[-0.04 f_{11}, -0.02 f_{11}]$. In between these frequencies, the bounds of the error vary linearly with respect to k and l. The center of the interval is not zero for frequencies other than the first, due to the error between thin- and thick-plate theories.

C. Identification Methods

The least-squares method minimizes the objective function shown in Eq. (17), where $f_{kl}^{\text{resp}}(E_x, G_{xy})$ is the response calculated from Eq. (14), using the mean values of a, b, h, and ρ:

$$J(E_x, G_{xy}) = \sum_{k,l=1,\ldots,3} (f_{kl}^{\text{resp}}(E_x, G_{xy}) - f_{kl}^{\text{meas}})^2 \tag{17}$$

For the experimental measurements we assume we know the average of the systematic error $(a_{kl} + b_{kl})/2$, for which we correct each

Table 12 Simulated measured frequencies and true frequency values (without measurement error)

	Frequency, Hz								
	f_{11}	f_{12}	f_{13}	f_{21}	f_{22}	f_{23}	f_{31}	f_{32}	f_{33}
Measured	267.9	612.9	1266.3	863.6	1070.5	1594.4	1892.0	2032.5	2409.1
True	268.3	612.7	1267.4	864.5	1068.7	1593.9	1893.6	2030.1	2412.3

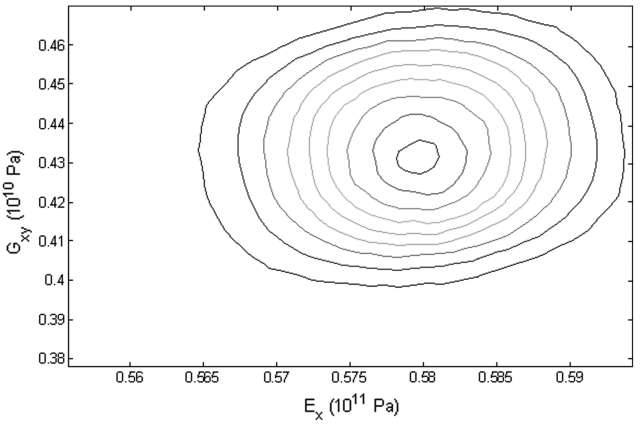

Fig. 2 Posterior (E_x, G_{xy}) distribution found with the Bayesian approach.

experimental frequency f_{kl}^{meas}. This is a significant assumption in favor of the least-squares approach. In reality, the systematic error might be less well known, which could bias the results. On the other hand, the Bayesian approach can handle even vague information on the systematic error, as we will show in the next paragraphs.

The Bayesian approach can be written, as shown in Eq. (18):

$$\pi_{\{E_x,G_{xy}\}/\{f_{11},\ldots,f_{33}\}=\{f_{11}^{\text{meas}},\ldots,f_{33}^{\text{meas}}\}}(\{E_x, G_{xy}\}) = \tfrac{1}{K}\pi_{\{f_{11},\ldots,f_{33}\}/\{E_x,G_{xy}\}}(\{f_{11}^{\text{meas}},\ldots,f_{33}^{\text{meas}}\}) \cdot \pi^{\text{prior}}_{\{E_x,G_{xy}\}}(\{E_x, G_{xy}\}) \tag{18}$$

A main difference compared to the three-bar truss is that we now also have measurement and modeling error, which we can take into account in the Bayesian approach. We assume that we know there is some numerical noise and that thin-plate theory overpredicts the natural frequency, but we assume we do not know the exact amount. Accordingly we assume the following frequency and error model for the Bayesian identification:

$$f_{kl} = f_{kl}^{\text{resp}}(\{E_x, G_{xy}\}, \boldsymbol{p}) + \tilde{u}_{kl} \tag{19}$$

where f^{resp} is the model response using Eq. (14), $\{E_x, G_{xy}\}$ are the values of the material properties considered at each identification step, and $\boldsymbol{p}$ are simulated values of the other input parameters a, b, h, and ρ. Variable $\tilde{\boldsymbol{u}}$ is a random variable uniformly distributed in the interval $[\tilde{a}_{kl}, \tilde{b}_{kl}]$, where $\tilde{a}_{kl}$ and $\tilde{b}_{kl}$ are obtained using Eq. (16) with $a_{lb} = -5 \times 10^{-3}$, $a_{ub} = -5 \times 10^{-2}$, $b_{lb} = 5 \times 10^{-3}$, and $b_{ub} = -1 \times 10^{-2}$. Note that these error bounds are significantly wider than those used for simulating the experiment (see previous subsection), reflecting the fact that we only have vague knowledge of the error model, and we tend to be conservative.

Note that the joint frequency distribution is of unknown shape because the frequency response is nonlinear in the uncertain input parameters $\boldsymbol{p}$, preventing an analytical calculation of the joint normal PDF and thus of the likelihood function. Instead, for this particular case, in which we assumed a uniformly distributed error, we use an alternative likelihood calculation approach by integrating the simulated frequencies PDF between the error bounds, as shown in Eq. (20):

$$\pi_{f/\{E_x,G_{xy}\}}(\boldsymbol{f}^{\text{meas}}) = \frac{1}{K}\int_{\boldsymbol{f}^{\text{meas}}-\tilde{\boldsymbol{a}}}^{\boldsymbol{f}^{\text{meas}}+\tilde{\boldsymbol{b}}} \pi_{f^{\text{MC}}/\{E_x,G_{xy}\}}(\boldsymbol{f}^{\text{input}_{\text{MC}}})\, \boldsymbol{d}\boldsymbol{f}^{\text{input}_{\text{MC}}} \tag{20}$$

where $\boldsymbol{f}$ is the nine-dimensional random variable of the frequency measurement prediction; $\boldsymbol{f}^{\text{meas}}$ is the nine-dimensional vector of the measured frequencies; $\tilde{\boldsymbol{a}}$ and $\tilde{\boldsymbol{b}}$ are the nine-dimensional vectors of the measurement uncertainty bounds $\tilde{a}_{kl}$ and $\tilde{b}_{kl}$; K is a normalizing constant; and $\boldsymbol{f}^{\text{input}_{\text{MC}}} = f_{kl}^{\text{resp}}(\{E_x, G_{xy}\}, \boldsymbol{p})$ is the nine-dimensional random variable of the frequencies, due only to uncertainty on input parameters $\boldsymbol{p}$, and obtained by Monte Carlo simulation on the frequency expression of Eq. (14), with the input uncertainties of Table 11.

Equation (20) is equivalent to saying that the likelihood of measuring the frequencies $\boldsymbol{f}^{\text{meas}}$ is equal to the probability that the simulated frequencies $\boldsymbol{f}^{\text{input}_{\text{MC}}}$ fall inside the measurement uncertainty bounds. The integral in Eq. (20) is evaluated by counting the number of frequencies within the bounds $[\boldsymbol{f}^{\text{meas}} - \tilde{\boldsymbol{a}}, \boldsymbol{f}^{\text{meas}} + \tilde{\boldsymbol{b}}]$, out of the total number of simulated frequencies $\boldsymbol{f}^{\text{input}_{\text{MC}}}$. We used 50,000 Monte Carlo simulations. The present calculation approach can also be seen as implicitly using the independence of the measurement uncertainty and of the uncertainty due to input parameters, which allows reducing cost by avoiding the calculation of the full histogram (see [23] for more details on Eq. (20) and the use of the independence of random variables).

The prior distribution for the Bayesian identification was assumed to be a truncated, uncorrelated, binormal distribution with a mean of 57 GPa and a standard deviation of 10 GPa for E_x and 4.2 and 1.5 GPa, respectively, for G_{xy}. The distribution was truncated for E_x at 55.5 and 59.4 GPa and for G_{xy} at 37.8 and 47 GPa. The truncation bounds were chosen around the mean value of the prior and iteratively reduced, to lower computational cost, so that they eventually cover about five standard deviations of the posterior PDF. As for the three-bar truss case, the prior was chosen wide enough so that it does not provide any significant unfair advantage to the Bayesian approach.

D. Results

To illustrate the benefits of the Bayesian method, we first present the results for a randomly simulated experiment. The simulated measured frequencies are given in Table 12, together with the true frequency response (i.e., without the measurement error). When repeating the simulation of measured frequencies a few times, we found that the frequencies of Table 12 lead to rather high differences between the Bayesian and the least-squares approaches. This case can then be considered to be an extreme case. We also subsequently provide the average performance over 100 repetitions of the simulated experimental frequencies.

The results for the extreme case are presented in Table 13. The Bayesian approach identifies the distribution shown in Fig. 2.

Both approaches found an accurate E_x (about 1% error). However, for G_{xy}, the least-squares has more than 8% error, compared to 0.9% error for the Bayesian method. Furthermore, the Bayesian approach provides additional information in form of the distribution shown in Fig. 2 (notably, the standard deviation of the properties identified). The distribution of G_{xy} is much wider than that of E_x (note the different scales in Fig. 2), meaning that the confidence in the most likely value of G_{xy} is much poorer than in that of E_x. This reflects the well-known fact that G_{xy} is harder to identify accurately than is E_x from a vibration test.

The average performance over 100 repetitions of the identification with randomly simulated experiments is given in Table 14. The two methods are comparable for E_x, but the Bayesian approach is about 1.9 times more accurate for G_{xy}.

Table 14 Average performance for the plate-vibration problem with 100 repetitions

	Mean value, GPa	Standard deviation, GPa
Least-squares	$E_x = 57.5$; $G_{xy} = 4.26$	For E_x: 0.65 (1.13%) ; for G_{xy}: 0.15 (3.63%)
Bayesian	$E_x = 57.5$; $G_{xy} = 4.26$	For E_x: 0.50 (0.88%) ; for G_{xy}: 0.083 (1.96%)

VI. Conclusions

We compared two approaches to parameter identification for two examples: a basic least-squares approach and a statistical approach, the Bayesian method. Using a simple three-bar truss example we identified the following conditions under which the basic least-squares method is systematically outperformed by the Bayesian statistical approach: 1) different sensitivity of the response components to the parameters to be identified, 2) different uncertainty in the measurements, and 3) high correlation among the response components. The ratio of the accuracy of the two approaches depends on the specific problem, but for the truss problem, we illustrated that it can reach a factor of 10 when all the effects add up.

We then considered the identification of elastic constants from natural frequencies of a plate. Using simulated experiments affected by uncertainty in input parameters, measurement noise, and model error, we found that the Bayesian approach was more accurate, especially for identifying the shear modulus, which is typically a harder-to-identify property of composites.

A final advantage of the Bayesian approach is that it identifies the probability density function of the properties. This uncertainty quantification can benefit reliability-based design and optimization by allowing narrower safety margins, due to the improved uncertainty knowledge on the material properties.

Appendix A: Tutorial Explanation of the Bayesian Procedure on the Truss Example

To illustrate the Bayesian procedure used and, in particular, the construction of the likelihood function, we will consider a simple case in which all quantities are one-dimensional ($m = n = 1$, see the notations in Sec. II.A). We consider the three-bar truss problem, in which we have a single property to be identified (Young's modulus E) and a single measurement (the strain in bar C).

Applied to the present case, Eq. (8) of the Bayesian formulation can be written as

$$\pi_{E/\varepsilon_C=\varepsilon_C^{\text{meas}}}(E) = \tfrac{1}{K}\pi_{\varepsilon_C/E}(\varepsilon_C^{\text{meas}}) \cdot \pi_E^{\text{prior}}(E) \tag{A1}$$

That is, the distribution of E (given that in bar C we measured $\varepsilon_C^{\text{meas}}$) is equal to a normalization constant times the likelihood function of E (given that we measured $\varepsilon_C^{\text{meas}}$) times the prior distribution of E. The prior distribution used here is the same wide distribution described in Sec. III.D.

Next, we describe the likelihood function and its construction in more detail. This function provides an estimate of the likelihood of different modulus values, given the test result. Seen as a function of E, we can construct it point by point. That is, we fix an E successively from $-\infty$ to ∞ and calculate $\pi_{\varepsilon_C/E=E^{\text{fixed}}}(\varepsilon_C^{\text{meas}})$. As mentioned in Sec. III.D, infinity is truncated to reasonable bounds for the properties to be identified. For example, let us fix $E = 5$ GPa. We substitute this E back into Eq. (10) and propagate the uncertainties in the loads p and r in the same formula. This can be done analytically here, since the strains are linear in the loads, but Monte Carlo simulation can be used in the general case. Thus, we obtain $\pi_{\varepsilon_C/E=5\ \text{GPa}}(\varepsilon_C)$, the distribution function of ε_C, if E is 5 GPa and given the uncertainties in p and r (see Fig. A1).

We note that if E were 5 GPa, the strain in bar C would be double its value, as for an E of 10 GPa. That is, $\pi_{\varepsilon_C/E=5\ \text{GPa}}(\varepsilon_C)$ is centered around -5.27 mε, compared to the value of -2.87 mε, which is the actual (measured) strain in the bar with the true E of 10 GPa and the true values of loads (different from the mean values, involved in this likelihood calculation).

Looking back at the construction of the likelihood function, we need to take the distribution $\pi_{\varepsilon_C/E=5\ \text{GPa}}(\varepsilon_C)$ at the point $\varepsilon_C = \varepsilon_C^{\text{meas}}$; that, is we need to compute $\pi_{\varepsilon_C/E=5\ \text{GPa}}(\varepsilon_C^{\text{meas}})$. From Fig. A1 we can see that this point is located in the tail of the distribution $\pi_{\varepsilon_C/E=5\ \text{GPa}}(\varepsilon_C)$, so the corresponding value of $\pi_{\varepsilon_C/E=5\ \text{GPa}}(\varepsilon_C^{\text{meas}})$ will be relatively low. That means that the likelihood is relatively low that we will measure $\varepsilon_C^{\text{meas}} = -2.87$ mε if E is 5 GPa.

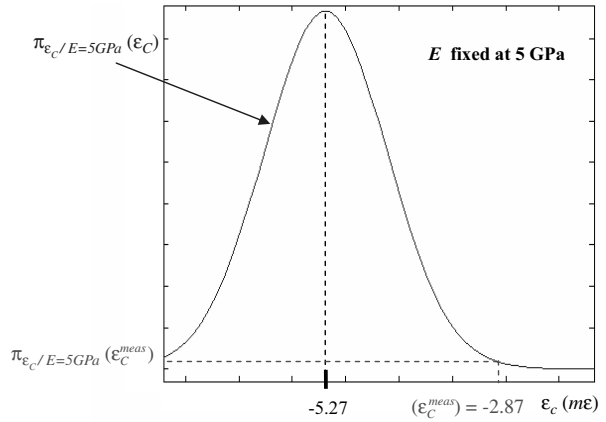

Fig. A1 Likelihood value using the distribution of ε_C if E were 5 GPa.

Now let us assume that we fix $E = 9.18$ GPa and repeat the same procedure. In this case we will obtain a distribution similar to that in Fig. A1, except that it will be centered in -2.87 mε. This means that the point $\pi_{\varepsilon_C/E=9.18\ \text{GPa}}(\varepsilon_C^{\text{meas}})$ is the highest point on the distribution, so the likelihood that we measure $\varepsilon_C^{\text{meas}} = -2.87$ mε if E was 9.18 GPa is the highest.

In the same way, we can compute $\pi_{\varepsilon_C/E=E^{\text{fixed}}}(\varepsilon_C^{\text{meas}})$ for a series of E^{fixed} values within the truncation bounds with a given infinitesimally small step. If we do this, we obtain $l(E) = \pi_{\varepsilon_C/E}(\varepsilon_C^{\text{meas}})$, the likelihood function of E given $\varepsilon_C^{\text{meas}}$, which is a function of E and is plotted in Fig. A2. As previously mentioned, the most likely value of E given only the measurement in bar C is $E = 9.18$ GPa.

Had we used the nominal values of the loads and $\varepsilon_C^{\text{meas}} = -2.87$ mε, substituted these values back into Eq. (10) and solved for E, we would obtain $E = 9.18$ GPa. It is logical then that we find that 9.18 GPa is the most likely value for Young's modulus, since we assumed that the nominal values for the loads are the most likely ones. However, we considered an unlucky case here, in which the true values of the loads fell 2σ away from their mean values, which explains why 9.18 GPa is far from 10 GPa, the actual Young's modulus of the bars.

Note that even though the likelihood function is centered in 9.18 GPa, there is a small but nonnegligible probability that Young's modulus is around 10 GPa (cf. Fig. A2). The true value of 10 Gpa is actually about 2σ away from the mean value of 9.18 GPa, which seems logical since the true values of the loads were 2σ away from their mean.

At this point we can finalize the Bayesian procedure. We have the prior distribution of E that we defined in Sec. III.D. We have just

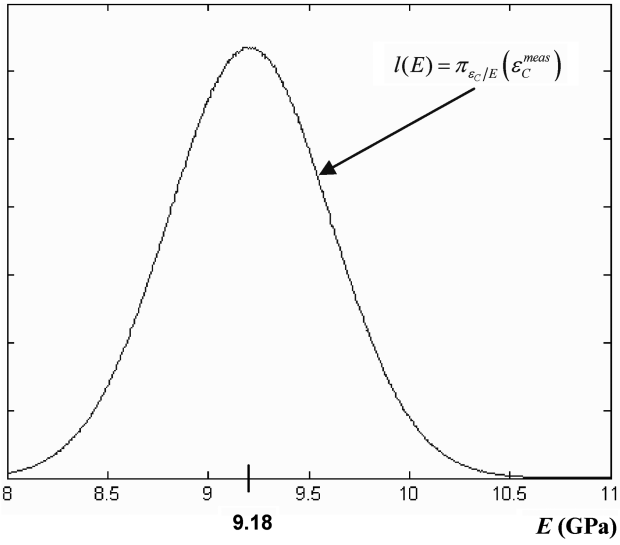

Fig. A2 Likelihood function of E given $\varepsilon_C^{\text{meas}}$.

calculated the likelihood function of E given $\varepsilon_C^{\text{meas}}$ (see Fig. A2); all that remains is to apply the Bayesian formulation of Eq. (A1): that is, multiply the two functions and normalize the resulting distribution. This is the probability distribution of the identified Young's modulus given that we measured, $\varepsilon_C^{\text{meas}}$.

If we have more than one parameter to identify, we have to define a joint probability distribution for the prior. This is illustrated on the vibration problem. The construction of the likelihood function would also be more time-consuming, since instead of describing an interval point by point, we would have to describe a surface.

If we have multiple measurement points (for example, strains in each of the bars), we would have to consider the joint probability distribution of the measurements and evaluate it at the measurement point when constructing the likelihood function. This is illustrated on both the vibration problem and the three-bar truss in Secs. IV and V.

Appendix B: Least-Squares Implicit Weighting According to Response Sensitivity

Here, we provide the proof of the statement of Sec. IV.B: the basic least-squares formulation implicitly assigns more weight to quantities that have high sensitivity with respect to the parameter to be identified.

For simplicity, we consider only linear models of the quantity to be identified, under the form $\boldsymbol{y} = Ax$ (same notations as in Sec. II). In this case, the least-squares formulation can be written as shown in Eq. (B1):

$$x^* = \arg\min_x J(x) \tag{B1}$$

where

$$J(x) = \tfrac{1}{2}(Ax - \boldsymbol{y}^{\text{meas}})^T(Ax - \boldsymbol{y}^{\text{meas}})$$

Since J is convex in x, the solution stems from solving $\nabla J(x) = 0$. The solution x^* is then found by solving the normal equations:

$$A^T A x^* = A^T \boldsymbol{y}^{\text{meas}} \tag{B2}$$

and $A^T A$ is usually invertible when $m > n$ (see the notations in Sec. II.A). The normal equations can also be written as

$$A^T(Ax^* - \boldsymbol{y}^{\text{meas}}) = 0 \tag{B3}$$

which shows that in the space of the measurements $\boldsymbol{y}$, the residual vector $Ax^* - \boldsymbol{y}^{\text{meas}}$ is perpendicular to the model surface whose directing vectors are A^i. This also means that the solution x^* to the basic least-squares formulation of Eq. (B1) is obtained by projecting the experimental measurement point $\boldsymbol{y}^{\text{meas}}$ onto the model surface $\boldsymbol{y} = Ax$. This is illustrated in Fig. B1 when $m = 2$ and $n = 1$.

To find how different measurements are weighted, we also obtain solutions based on a single measurement (this is possible since $n = 1$). The solution for measurement i is

$$x^{*i} = \arg\min_x \tfrac{1}{2}(A_i x - \boldsymbol{y}_i^{\text{meas}})^2 \quad \text{for } i = 1, \ldots, m \tag{B4}$$

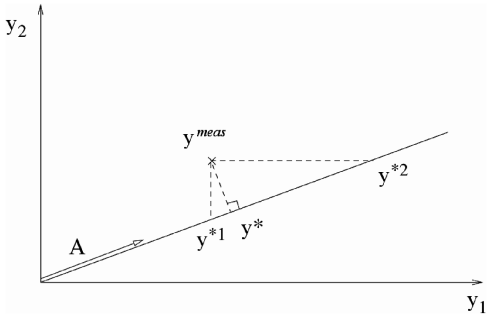

Fig. B1 Illustration of least-squares solution $\boldsymbol{y^* = Ax^*}$ and partial solutions $\boldsymbol{y^{*i}}$ for $\boldsymbol{m = 2}$ and $\boldsymbol{n = 1}$.

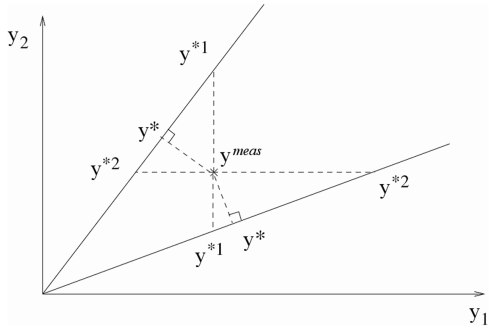

Fig. B2 Illustration of least-squares solution $\boldsymbol{y^* = Ax^*}$ and virtual measurements $\boldsymbol{y^{*i}}$ for two different slopes $\boldsymbol{A}$. In one case, the basic least-squares formulation assigns more weight to $\boldsymbol{y^{*1}}$, in the other case, it assigns more weight to $\boldsymbol{y^{*2}}$.

where subscript i represents the ith line of the respective matrix/vector. Accordingly, x^{*i} is the parameter found when only the measurement $\boldsymbol{y}_i^{\text{meas}}$ was used and $\boldsymbol{y}^{*i}$ was the corresponding value on the surface of the response: $\boldsymbol{y}^{*i} = Ax^{*i}$. We call x^{*i} the partial solutions and $\boldsymbol{y}^{*i}$ the corresponding virtual measurements, which are the projections, along the ith component, of $\boldsymbol{y}^{\text{meas}}$ onto the model surface $\boldsymbol{y} = Ax$ (see Fig. B1).

We can now investigate how the least-squares solution $\boldsymbol{y}^*$ depends on the virtual measurements $\boldsymbol{y}^{*i}$ and thus on the partial solutions x^{*i}. If $\boldsymbol{y}^*$ is closer to $\boldsymbol{y}^{*i}$, this can be seen as the least-squares procedure implicitly assigning more weight to $\boldsymbol{y}^{*i}$. Figure B2 illustrates two cases with different slopes. In the case in which y_1 is more sensitive to E variations than is y_2 (low slope in the y_1–y_2 plane), then the basic least-squares formulation assigns more weight to $\boldsymbol{y}^{*1}$ and the inverse. We can deduce that which partial solution is assigned more weight depends on the sensitivity of the response to the parameter to be identified. Mathematically, this can be quantified by $\partial x^*/\partial y_i^{\text{meas}}$. Deriving the normal Eq. (B2), we obtain

$$A^T A \frac{\partial x^*}{\partial y_i^{\text{meas}}} = A_i^T \tag{B5}$$

From Eq. (B5) we can deduce that the sensitivity of the identified parameters to the ith experiment depends on the ith line of A.

After this proof in a general case, it is interesting to analyze how the least-squares and the Bayesian approaches are represented graphically for the three-bar truss example. In Fig. B3 we illustrate the case studied in Sec. IV.B of different strain sensitivity to E, which translates into different strain magnitudes. The line is the model surface $\boldsymbol{y} = Ax$. In our case, $x = 1/E$ and $\boldsymbol{y} = \{\varepsilon_A, \varepsilon_B\}^T$. The circle is the experimental measurement and its orthogonal projection on the model surface (cross) is the least-squares identified modulus, $E = 9.67$ GPa. The center of the ellipses, $E^*_{\text{Bayes}} = 9.97$ GPa, is the Bayesian-identified modulus. The ellipses represent the joint strain distribution function $\pi_{\{\varepsilon_A,\varepsilon_B\}/E=9.97\ \text{GPa}}(\{\varepsilon_A, \varepsilon_B\})$ due to the uncertainties in the loads. If we vary E, this is the distribution leading to the highest likelihood of the experimental measurement, meaning that if we translate the distribution along the model surface, this is the distribution for which the outer ellipse gets the closest to the experimental point. Note that this explanation does not take into account the impact of the prior, which we have shown to be negligible in our case (see Sec. IV.E), because we have chosen a wide prior.

Figure B3 also helps understand why the basic least-squares formulation leads to poor results in the case of different sensitivity to E (i.e., different strain magnitude). Because of the different sensitivity to E, the model surface (line) has a low slope. The uncertainties in the loads propagate to the same relative uncertainties in the two strains, but different absolute uncertainties, due to the different strain magnitudes, meaning that the joint strain distribution will be elliptical instead of circular. The low slope in combination with the elliptical distribution leads the orthogonal projection of the measurement to be relatively far away from the maximum likelihood point, as illustrated in Fig. B3.

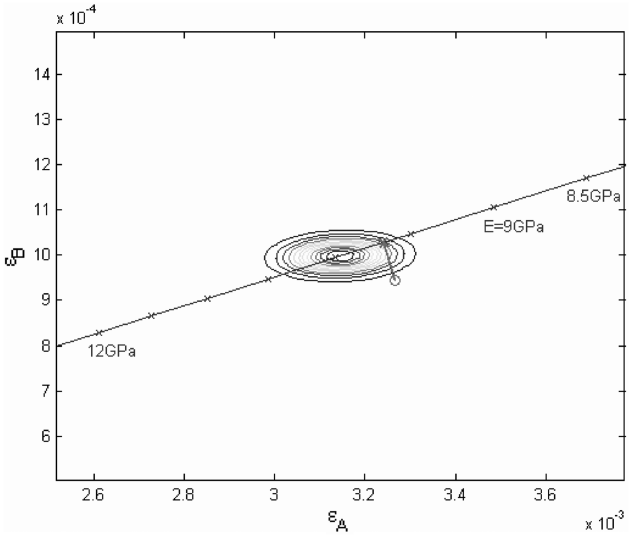

Fig. B3 Graphical representation of the least-squares and Bayesian results for the three-bar truss example for the different-sensitivity case (i.e., different strain magnitude). The circle is the experimental measurement, its orthogonal projection (cross) is the least-squares identified modulus, and the center of the ellipses is the Bayesian-identified modulus. The ellipses represent the contour plot of the strain distribution $\pi_{\{\varepsilon_A,\varepsilon_B\}/E=E^*_{\text{Bayes}}}(\{\varepsilon_A,\varepsilon_B\})$.

Appendix C: Bayesian and Least-Squares Behavior with Respect to Different Response Uncertainty

Similar to the graphical representation provided in Appendix B for different response sensitivity, we now provide an interpretation of the three-bar truss results in the case of different response uncertainty. Figure C1 illustrates the case studied in Sec. IV.C of different uncertainty in the loads, which propagates to different uncertainty in the strains. We have here the same sensitivity of the strains to Young's modulus, which can be seen by the 45° slope of the model surface. Note also that the elliptical shape of the joint strain distributions this time is not due to different strain sensitivity as in Appendix B, but to different uncertainties in the loads, which propagate to a higher uncertainty in ε_A than in ε_B.

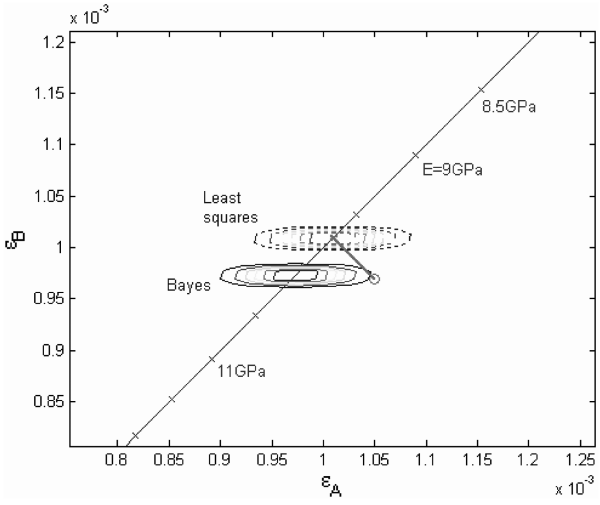

Fig. C1 Graphical representation of the least-squares and Bayesian results for the three-bar truss example for the different-uncertainty case. The circle is the experimental measurement, and its orthogonal projection (cross) is the least-squares identified modulus. The ellipses are the contour plot of the strain distribution $\pi_{\{\varepsilon_A,\varepsilon_B\}/E=E^*_i}(\{\varepsilon_A,\varepsilon_B\})$, where E^*_i is the least-squares identified modulus E^*_{LS} (dashed ellipses) or the Bayesian-identified modulus E^*_{Bayes} (full-line ellipses).

In addition to the joint strain distribution centered in the Bayesian-identified modulus (full-line ellipses), we also provide what the distribution would be if the modulus was the one found by the least-squares approach. This shows that the experimental measurement has a maximum likelihood on the strain distribution with the Bayesian modulus; i.e., the measurement point is the closest possible to the outer most ellipse of all possible distributions translated along the model surface line. In particular, the strain distribution centered in the least-squares modulus has a significantly lower likelihood.

Acknowledgments

The authors gratefully acknowledge financial support by the NASA Constellation University Institutes Program (CUIP) [formerly University Research, Engineering and Technology Institutes (URETI)] grant NCC3-994 to the Institute for Future Space Transport (IFST) at the University of Florida. The responsible Program Managers are Claudia Meyer and Jeffry Rybak at NASA John H. Glenn Research Center at Lewis Field.

References

[1] Rust, S. W., Todt, F. R., Harris, B., Neal, D., and Vangel, M., "Statistical Methods for Calculating Material Allowables for MIL-HDBK-17," *Test Methods and Design Allowables for Fibrous Composites*, edited by C. C. Chamis, ASTM International, West Conshohocken, PA1989, pp. 136–149.

[2] Bjorck, A., *Numerical Methods for Least Squares Problems*, Society for Industrial and Applied Mathematics, Philadelphia, 1996.

[3] Lawson, C. L., and Hanson, R. J., *Solving Least Squares Problems*, Prentice–Hall, Englewood Cliffs, NJ, 1974.

[4] Tarantola, A., *Inverse Problem Theory and Model Parameter Estimation*, Society for Industrial and Applied Mathematics, Philadelphia, 2005.

[5] Rouger, F., Khebibeche, M., and Govic, C., "Non-Determined Tests as a Way to Identify Wood Elastic Parameters: The Finite Element Approach," *Proceedings of the EUROMECH Colloquium 269 Mechanical Identification of Composites*, Elsevier, New York, 1990, pp. 82–90.

[6] Magorou, L. L., Bos, F., and Rouger, F., "Identification of Constitutive Laws for Wood-Based Panels by Means of an Inverse Method," *Composites Science and Technology*, Vol. 62, No. 4, 2002, pp. 591–596.
doi:10.1016/S0266-3538(01)00149-X

[7] Molimard, J., Le Riche, R., Vautrin, A., and Lee, J., "Identification of the Four Orthotropic Plate Stiffnesses Using a Single Open-Hole Tensile Test," *Experimental Mechanics*, Vol. 45, No. 5, 2005, pp. 404–411.
doi:10.1007/BF02427987

[8] Genovese, K., Lamberti, L., Pappalettere, C., "Improved Global–Local Simulated Annealing Formulation for Solving Non-Smooth Engineering Optimization Problems," *International Journal of Solids and Structures*, Vol. 42, No. 1, 2005, pp. 203–237.
doi:10.1016/j.ijsolstr.2004.07.015

[9] Frederiksen, P. S., "Experimental Procedure and Results for the Identification of Elastic Constants of Thick Orthotropic Plates," *Journal of Composite Materials*, Vol. 31, No. 4, 1997, pp. 360–382.

[10] Sol, H., "Identification of Anisotropic Plate Rigidities," Ph.D. Dissertation, Vrije Universiteit, Brussels, 1986.

[11] Maletta, C., and Pagnotta, L., "On The Determination of Mechanical Properties of Composite Laminates Using Genetic Algorithms," *International Journal of Mechanics and Materials in Design*, Vol. 1, No. 2, 2004, pp. 199–211.
doi:10.1007/s10999-004-1731-5

[12] Shi, Y., Sol, H., and Hua, H., "Transverse Shear Modulus Identification by an Inverse Method Using Measured Flexural Resonance Frequencies from Beams," *Journal of Sound and Vibration*, Vol. 285, Nos. 1–2, 2005, pp. 425–442.
doi:10.1016/j.jsv.2004.03.074

[13] Isenberg, J., "Progressing from Least-Squares to Bayesian Estimation," *Proceedings of the ASME Design Engineering Technical Conferences*, American Society of Mechanical Engineers, New York, 1979, pp. 71–82.

[14] Daghia, F., De Miranda, S., Ubertini, F., and Viola, E., "Estimation Of Elastic Constants of Thick Laminated Plates Within a Bayesian Framework," *Composite Structures*, Vol. 80, No. 3, 2007, pp. 461–473.
doi:10.1016/j.compstruct.2006.06.030

[15] Marwala, T., and Sibisi, S., "Finite Element Model Updating Using Bayesian Framework and Modal Properties," *Journal of Aircraft*, Vol. 42, No. 1, 2005, pp. 275–278. doi:10.2514/1.11841

[16] Alvin, K. F., "Finite Element Model Update Via Bayesian Estimation and Minimization of Dynamic Residuals," *AIAA Journal*, Vol. 35, No. 5, 1997, pp. 879–886. doi:10.2514/2.7462

[17] Beck, J. L., and Katafygiotis, L. S., "Updating Models and Their Uncertainties. I: Bayesian Statistical Framework," *Journal of Engineering Mechanics*, Vol. 124, No. 4, 1998, pp. 455–461. doi:10.1061/(ASCE)0733-9399(1998)124:4(455)

[18] Elseifi, M. A., "Bayesian Models for Updated Cured Composite Properties," 43rd AIAA/ASME/ASCE/AHS/ASC Structures, Structural Dynamics, and Materials Conference, AIAA Paper 2002-1273, Denver, CO, 2002.

[19] Dascotte, E., "Identification of Random Material Properties Using a Mixed Deterministic-Probabilistic Method," *Proceedings of the International Seminar on Modal Analysis*, Leuven, Belgium, 2004, pp. 20–22.

[20] Rebba, R., and Mahadevan, S., "Statistical Methods for Model Validation Under Uncertainty," 47th AIAA/ASME/ASCE/AHS/ASC Structures, Structural Dynamics, and Materials Conference, Newport, RI, AIAA Paper 2006-1997, 2006.

[21] Rebba, R., Mahadevan, S., and Huang, S., "Validation and Error Estimation of Computational Models," *Reliability Engineering and System Safety*, Vol. 91, Nos. 10–11, 2006, pp. 1390–1397.

[22] Gogu, C., Haftka, R. T., Le Riche, R., Molimard, J., Vautrin, A., and Sankar, B. V., "Bayesian Statistical Identification of Orthotropic Elastic Constants Accounting for Measurement and Modeling Errors," 11th AIAA Non-Deterministic Approaches Conference, AIAA Paper 2009-2258, Palm Springs, CA, 2009.

[23] Gogu, C., "Facilitating Bayesian Identification of Elastic Constants Through Dimensionality Reduction and Response Surface Methodology," Ph.D. Dissertation, Univ. of Florida, Gainesville, FL, and Ecole des Mines de Saint Etienne, Saint Etienne, France, 2009.

[24] Berger, J. O., *Statistical Decision Theory and Bayesian Analysis*, Springer, New York, 1985.

[25] Kaipio, J. P., and Somersalo, E., *Statistical and Computational Inverse Problems*, Springer, New York, 2005.

[26] Myers, R. H., and Montgomery, D. C., *Response Surface Methodology: Process and Product Optimization Using Designed Experiments*, 2nd ed., Wiley, New York, 2002.

[27] Ayyub, B. M., and Chia, C. Y., "Generalized Conditional Expectation for Structural Reliability Assessment," *Structural Safety*, Vol. 11, No. 2, 1992, pp. 131–146. doi:10.1016/0167-4730(92)90005-8

[28] Gürdal, Z., Haftka, R. T., and Hajela, P., *Design and Optimization of Laminated Composite Materials*, Wiley Interscience, New York, 1998.

R. Kapania
Associate Editor